Zhang, R.; Hong, X. (2022) Analysis of nutrient intake and energy consumption during college students' exercise based on big data technology. Revista Internacional de Medicina y Ciencias de la Actividad Física y el Deporte vol. 22 (85) pp. 283-302
DOI: https://doi.org/10.15366/rimcafd2022.85.018

ORIGINAL

Analysis of nutrient intake and energy consumption during college students' exercise based on big data technology

Runping Zhang[1], Xue Hong*[2]
[1]College of Physical Education, Sanya University, Sanyan, 572022, Hainan, China
[2]College of Digital Economy, Sanya University, Sanyan, 572022, Hainan, China
Email: andreaxue@126.com

UNESCO Code / UNESCO Code:
Council of Europe classification / Council of Europe classification:

Recibido 03 de enero de 2021**Received** January 03, 2021
Aceptado 13 de enero de 2022 **Accepted** January 13, 2022

Abstract

In order to analyze the correlation between nutrient intake and energy consumption in college students' exercise, this paper combines big data technology to analyze the nutrition intake and energy consumption in college students' exercise process, so as to promote the balance of nutrient intake and energy consumption in college students' exercise. Moreover, this paper proposes a data-driven model predictive controller for designing multi-rate sampling systems based on model regression and system identification. In addition, this paper uses an extended dimension method to transform the multi-rate sampling system into an equivalent linear discrete time-invariant system to perform model optimization. Finally, this paper verifies the validity of the model in this paper through experimental research and gives some suggestions.

Keywords. big data, college students' exercise, nutrition intake, energy consumption

1. INTRODUCTION

At present, the nutritional status of college students has aroused extensive attention from all walks of life, and it is necessary to further promote nutrition and health knowledge education by adopting various approaches and intensifying efforts. First of all, students should be assisted to establish a healthy concept, pay attention to a reasonable diet, and abandon unhealthy eating habits. Moreover, each region needs to combine the different eating habits of different regions, with the goal of improving the nutritional status of students, and encourage students to eat on time every day. At the same time, it is necessary to ensure the intake of daily nutrients, pay attention to the combination of meat and vegetables, and consume an appropriate number of

coarse grains such as millet, corn, and sorghum rice on the basis of adequate protein intake (Altwaijry, El-Masry, Alotaibi, Tousson, & Saleh, 2020). Secondly, it is necessary to increase the number of nutrition knowledge education courses, increase nutrition knowledge education and publicity activities, so that every student can realize the importance of nutrition knowledge. It needs to be suggested to set up nutrition and health education elective courses in college classrooms, hold a series of lectures, help college students establish good eating habits, and gradually form a nutrition and health education system for college students (Arman, Al Mahmud, Mahmud, & Reza, 2019).

In the process of implementing health education, some new ideas can be introduced. Its core concept is, according to the relevant content in the residents' dietary guidelines, to introduce the concept of balanced diet to college students by using PSBH methods and principles to urge college students to strengthen physical exercise through the characteristics of college students' diligent thinking and high attention to health problems, change their unreasonable lifestyles, and get enough sleep time. Specific methods include distributing nutrition and health publicity materials to college students, holding special lectures on nutrition knowledge, etc., to gradually improve the nutritional status of college students (Benzer, Kandemir, Kucukler, Comaklı, & Caglayan, 2018).

Increase the subsidies for the student canteen, reduce the price of dishes, improve the management level and service level of the canteen, ensure the sanitation and tidyness of the student canteen, increase the types of main and non-staple food in the canteen, extend the operating hours of the canteen, and provide students with more delicious dishes. Students' satisfaction with the canteen service encourages students to eat more in the canteen (Benzer et al., 2018).

The health administrative department and the education department jointly formulate guidance documents related to nutrition and health education for students, to increase the attention of the whole society to the nutritional status of students from the policy level, and to scientifically plan the development direction of nutrition work in the future (Beyfuss & Hood, 2018). Encourage and support the development of nutrition disciplines, set up nutrition majors in more medical colleges, and train more professional nutrition talents in combination with the current social needs for clinical nutrition, nutritional meals and other aspects (Choi, Liu, & Pan, 2018). Further improve the salaries of nutrition staff, improve the social recognition of nutrition professionals, and support the development of nutrition disciplines (Daenen et al., 2019).

The factors that produce body shape differences are very complex, whether it is diet, environment, training time, methods, coaches, etc., which will affect the body shape indicators of bodybuilders (Dzik & Kaczor, 2019). A large number of studies have shown that many factors such as age, geographical environment, society, genetics, gender, region, and weather also affect human body shape and physique (Forman & Zhang, 2021). Due to reasons such as training methods, strength, diet, etc., the gaps in the golden

ratio of different bodybuilders are also different (Feng et al., 2020). Differences in training methods can affect differences in body shape.

The selection of athletes is also an important factor affecting the further training of bodybuilding. By systematically and purposefully selecting talents with better conditions and suitable for a certain sport, it is easier to achieve excellent results (Garza-Lombó, Posadas, Quintanar, Gonsebatt, & Franco, 2018). There are many studies on the differences of morphological indicators by predecessors, but most of them focus on a certain angle, or describe them in a general manner, and do not discuss in depth. Nowadays, colleges and universities pay more and more attention to bodybuilding, and the body shape data of college bodybuilders are getting closer and closer to the professional level. The body shape indicators of professional bodybuilders and college bodybuilders are compared, and the reasons for the differences are analyzed. Professional training of college bodybuilders provides more reference data and suggestions (Hassanzadeh & Rahimmi, 2019).

Human health is determined by genetic, lifestyle and environmental factors. In addition to acute injuries, infectious diseases and environmental factors, the main threats to health come from chronic diseases (Kruk, Aboul-Enein, Kładna, & Bowser, 2019), the latter including overweight, obesity, cardiovascular and cerebrovascular diseases (coronary heart disease, stroke), type 2 diabetes, hypertension, malignant tumors , fatty liver and dyslipidemia, osteoporosis, etc.

The main risk factors for these chronic diseases (diseases) are lack of physical activity, unreasonable dietary structure (high protein, high fat, high calorie food, too little intake of cereals, vegetables and fruits, etc.) and unhealthy lifestyles such as excessive drinking. The health effects of exercise and nutrition on human body shape, cardiovascular function, skeletal muscle function, neuro-muscle motor unit function, metabolic function, etc. involve the mechanism of action at the overall, system, tissue, cellular and even molecular levels, often involving body weight and body weight. BMI, cardiopulmonary function, muscle strength and endurance, balance and coordination ability, material energy metabolism and insulin sensitivity, endoplasmic reticulum stress, etc. (Kurucz et al., 2018). Nutrition is the foundation of physical health, and malnutrition will inevitably damage the health of the body, which will have a great impact on life and learning. Therefore, universities must provide targeted guidance for the malnutrition of college students (Olechnowicz, Tinkov, Skalny, & Suliburska, 2018). For example, special nutrition courses are set up so that students can understand the importance of nutrition and have more awareness of the harm of nutritional imbalance. Let it actively change the quality and quantity of nutrient intake. The so-called reasonable nutrition has the following requirements: First, every day, all nutrients needed for healthy development of the body should be taken in, including protein, fat, various vitamins and trace elements. Second, try to choose foods that are easy to absorb and increase appetite. Third, to ensure the law of three meals a day, especially the intake of breakfast. Try to avoid eating foods that are harmful to your body (Xi et al., 2019). Fourth, don’t be picky eaters, don’t have a partial eclipse, and don’t

overeat, control your food intake, and stay away from the three high diseases of wealth. A balanced intake of various nutrients has a positive effect on the body (Qi & Dong, 2021). It can provide all kinds of necessary nutrients for the body to maintain the body temperature at a constant level, it can also regulate and control the normal life activities of the human body, and can perform necessary actions on the human body when the human body is attacked and injured. 's repair. Only by reasonably and scientifically ingesting various nutrients necessary for the body can the human body function better and ensure the healthy growth and development of college students. Only under balanced nutritional conditions can college students have more abundant physical strength and flexible brains to improve study and work efficiency and improve interpersonal relationships (Qi & Dong, 2021; Wei, Lu, Kang, & Song, 2020). This paper combines big data technology to analyze the nutritional intake and energy consumption of college students in sports, promote the balance of nutritional intake and energy consumption in college students' sports, and improve the sports health of college students.

2. Intelligent motion and energy data analysis system

The general multi-rate sampling system considered is as follows:

$$\begin{aligned}\dot{\tilde{x}}(t) &= A_c\tilde{x}(t) + B_c\tilde{u}(t)\\ \tilde{z}(t) &= C_{1c}\tilde{x}(t) + D_c\tilde{u}(t)\\ \tilde{y}(t) &= C_{2c}\tilde{x}(t) \quad (1)\end{aligned}$$

As the multi-rate feature described in the previous section, for system (1), the sampling intervals for measuring the q outputs are $n_1h, n_2h, \ldots, n_qh$ respectively. Similarly, the period intervals of the p zero-order retainers are $m_1h, m_2h, \ldots, m_p$ respectively, and *h* is a positive integer. The parameter N is the greatest common multiple of $m_1, m_2, \ldots, m_p, n_1, n_2, \ldots, n_q$. As can be seen from Section 2.2, for the processing of multi-rate sampling system, it can be discretized and then expanded into an equivalent linear discrete time-invariant system:

$$\begin{aligned}x(k+1) &= \bar{A}x(k) + \bar{B}\bar{u}(k)\\ \bar{z}(k+1) &= \bar{C}_1x(k) + \bar{D}_1\bar{u}(k)\\ \bar{y}(k) &= \bar{C}_2x(k) + \bar{D}_2\bar{u}(k) \quad (2)\end{aligned}$$

Its relevant parameters are as follows:

$$\bar{u}(N\tilde{k}) = \begin{bmatrix} u_1(N\tilde{k}) \\ u_2(N\tilde{k}) \\ \vdots \\ u_p(N\tilde{k}) \end{bmatrix}, \bar{u}_i(N\tilde{k}) = \begin{bmatrix} u_i(N\tilde{k}) \\ u_i(N\tilde{k}+m_i) \\ \vdots \\ u_i(N\tilde{k}+N-m_i) \end{bmatrix}$$

$$\bar{y}(N\tilde{k}) = \begin{bmatrix} y_1(N\tilde{k}) \\ y_2(N\tilde{k}) \\ \vdots \\ y_q(N\tilde{k}) \end{bmatrix}, \bar{u}_i(N\tilde{k}) = \begin{bmatrix} y_i(N\tilde{k}) \\ y_i(N\tilde{k}+n_i) \\ \vdots \\ y_i(N\tilde{k}+N-n_i) \end{bmatrix}$$

$$\bar{z}(N\tilde{k}) = \begin{bmatrix} z_1(N\tilde{k}) \\ z_2(N\tilde{k}) \\ \vdots \\ z_{n_z}(N\tilde{k}) \end{bmatrix}, \bar{u}_i(N\tilde{k}) = \begin{bmatrix} z_i(N\tilde{k}) \\ z_i(N\tilde{k}+1) \\ \vdots \\ z_i(N\tilde{k}+N-1) \end{bmatrix}$$

$$\bar{A} = A^N, \bar{B} = \begin{bmatrix} \bar{B}_1 & \bar{B}_2 & \cdots & \bar{B}_p \end{bmatrix}$$

$$\bar{B}_j = \begin{bmatrix} \sum_{q=1}^{m_j} A^{N-q} b_j & \cdots & \sum_{q=1}^{m_j} A^{m_j-q} b_j \end{bmatrix}$$

$$\bar{C}_1 = \begin{bmatrix} \bar{C}_{11} \\ \bar{C}_{12} \\ \vdots \\ \bar{C}_{1m_z} \end{bmatrix}, \bar{C}_{1j} = \begin{bmatrix} \bar{C}_{1j} \\ \bar{C}_{1i}A \\ \vdots \\ \bar{C}_{1j}A^{N-1} \end{bmatrix}, \bar{C}_{2j} = \begin{bmatrix} \bar{C}_{2j} \\ \bar{C}_{2j}A^{n_j} \\ \vdots \\ \bar{C}_{1j}A^{N-n_j} \end{bmatrix}$$

$$[\bar{D}_s]_{ij} = \begin{bmatrix} ([\bar{D}_s]_{ij})_{11} & ([\bar{D}_s]_{ij})_{11} & \cdots & ([\bar{D}_s]_{ij})_{11} \\ ([\bar{D}_s]_{ij})_{11} & ([\bar{D}_s]_{ij})_{11} & & \vdots \\ \vdots & & \ddots & \vdots \\ ([\bar{D}_s]_{ij})_{11} & \cdots & \cdots & ([\bar{D}_s]_{ij})_{11} \end{bmatrix}$$

$$([\bar{D}_s]_{ij})_{\alpha\beta} = [d_s]_{ij}\Theta(m_j - 1 - r)\Theta(r) + \Omega_d$$

$$\Omega_d = \sum_{q=0}^{m_j-1} \Theta(r-1-q)[c_s]_i A^q \psi(r-m_j) b_j$$

$$r = (\alpha-1)\frac{N}{n_i} - (\beta-1)\frac{N}{m_j}, 1 \le \alpha \le n_i, 1 \le \beta \le m_j$$

$$\Theta(q) = \begin{cases} 1(if\ q \ge 0) \\ 0(otherwise) \end{cases}, \psi(q) = \begin{cases} A^q(if\ q \ge 0) \\ 0(otherwise) \end{cases}$$

$$y = \begin{cases} n_z(if\ s=1) \\ q(if\ s=2) \end{cases}, v = \begin{cases} N(if\ s=1) \\ \frac{N}{m_i}(if\ s=2) \end{cases}$$

Among them, b_{nj} is the j-th column of matrix B_n, $[\bar{D}_s]_{ij}$ is the i row and j column elements of matrix $\bar{D}_{st}$, $[C_s]_i$ is the i-th row of matrix C_s, and $[b_t]_j$ is the j-th row of matrix B_t.

Then, the cost function of system (1) in this subsection is:

$$J(k) = \sum_{j=1}^{NM_y} \|y_{sp}(k+j) - y(k+j)\|_{\bar{Q}}^2 + \sum_{j=M_u+1}^{NM_u} \|\Delta u(k+j-1)\|_{\bar{R}}^2 \quad (4)$$

At the same time, it can meet the following constraints:

$$\begin{cases} u_{min} \le u(k+j) \le u_{max} \\ \Delta u_{min} \le u(k+j) \le \Delta u_{max} \\ y_{min} \le y(k+j) \le y_{max} \end{cases} \quad (5)$$

Similarly, $\bar{R}$ is another variable of the positive definite weight diagonal matrix. For details, please refer to the cost function of optimal control LQR. The MPC control structure of the multi-rate sampling system based on PLS is shown in Figure 1.

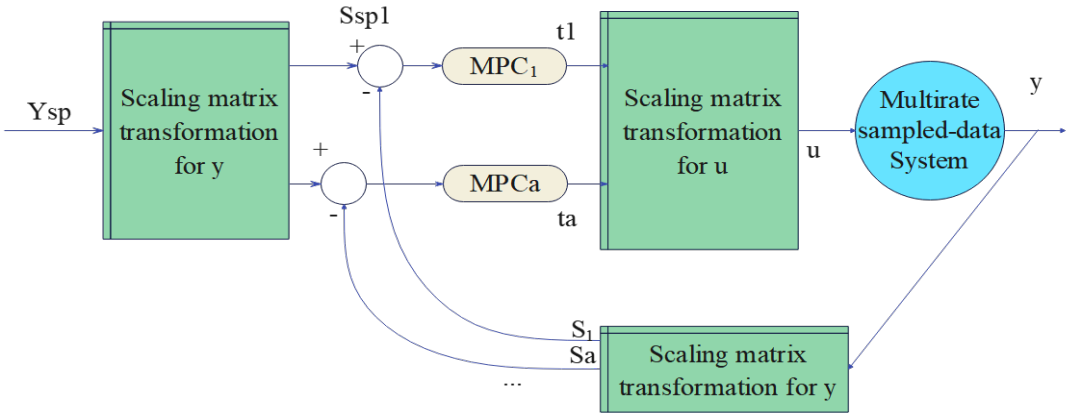

Figure 1. MPC control structure of multi-rate sampling system based on PLS

First, input and output data are collected for ngNh over a period of time through system (1). Then, the obtained data is recombined into n groups of input z and output y with the data structure of formula (3). At the same time, we define:

$$U_0 = \begin{bmatrix} \bar{u}^T(1) \\ \vdots \\ \bar{u}^T(n_1) \end{bmatrix}, Y_0 = \begin{bmatrix} \bar{y}^T(1) \\ \vdots \\ \bar{y}^T(n_1) \end{bmatrix} \quad (6)$$

This data structure is also the base structure for starting data analysis. Before principal component analysis of the data, the dataset needs to be quantified.

We define the scale matrices of U_0 and Y_0 as W_u and W_y, and their offset matrices as E_u and E_y. Therefore, there are:

$$U = (U_0 - E_u)W_u, Y = (Y_0 - E_y)W_y \quad (7)$$

Further, we start to perform principal component analysis on the data U and Y, and we can get:

$$U = t_1 p_1^T + t_2 p_2^T + \cdots + t_a p_a^T + E_{a+1} = TP^T + E_{a+1}$$
$$Y = s_1 q_1^T + t_2 q_2^T + \cdots + s_a q_a^T + F_{a+1} = SQ^T + F_{a+1} \quad (8)$$

Here is to project U and Y in different directions until the projection cannot be continued. It can be seen that T and S are scoring matrices, that is,

metrics, and their load matrices, that is, projection direction matrices are P and O.E_{a+1} and F_{a+1} are the residual matrix of U and Y after multiple projections. a is the number of principal components and the number of projections.

In the field of partial least squares, the combined autoregressive exogenous (ARX) model structure is a commonly used model in the field of multivariate model regression. The ARX model is defined as follows:

$$s_i(k) = [s_i(k-1), \cdots, s_i(k-j_a), t_i(k-1), \cdots, t_i(k-j_b)]h_i + \xi_i(k) = \alpha_i(k)h_i + \xi_i(k) = H_i(\alpha_i) \quad (9)$$

$H_i(\alpha_i)$ is the ARX model of the multi-rate sampling system. α_i is the regression variable. h_i is the parameter of the ARX model, and these parameters need to use the data sets U and Y for analysis and regression.

On the basis of ARX model (9) and principal component analysis (8), the dynamic model of the data-driven multi-rate sampling system can be obtained:

$$\hat{Y} = H_1(\alpha_1)q_1^T + H_2(\alpha_2)q_2^T + \cdots + H_a(\alpha_a)q_a^T = H(\alpha)Q^T \quad (10)$$

Among them, $H(\alpha) = [H_1(\alpha_1)q_1^T + H_2(\alpha_2)q_2^T + \cdots + H_a(\alpha_a)q_a^T]$, and $\hat{Y}$ is the estimated values of variable Y.

For the cost function (4), through the ARX model of the above-mentioned PLS method regression and the multi-rate expansion method, it can be found that it is equivalent to the following formula:

$$\bar{J}(k) = \sum_{j=1}^{M_y} \left\| \bar{y}_{sp}(k+j) - \bar{y}(k+j) \right\|_{\bar{Q}}^2 + \sum_{j=2}^{M_u} \left\| \Delta\bar{u}(k+j-1) \right\|_{\bar{R}}^2 \quad (11)$$

At the same time, it can satisfy the following constraints:

On the basis of formula (8), when $n_1 = 1$, there are the following formula transformations:

$$\begin{aligned} &\left\| \bar{y}_{sp}(k+j) - \bar{y}(k+j) \right\|_{\bar{Q}}^2 \\ &= \left(\bar{y}_{sp}(k+j) - \bar{y}(k+j) \right)^T \bar{Q} \left(\bar{y}_{sp}(k+j) - \bar{y}(k+j) \right) \\ &= \left(Y_{sp}(k+j) - Y(k+j) \right) \bar{Q} \left(Y_{sp}(k+j) - Y(k+j) \right)^T \\ &= \left(S_{sp}(k+j) - S(k+j) \right) Q^T \bar{Q} Q \left(S_{sp}(k+j) - S(k+j) \right)^T \\ &= \left\| S_{sp}(k+j) - S(k+j) \right\|_{Q_1}^2 \end{aligned} \quad (12)$$

Using a similar approach, the following relationship can be easily obtained:

$$\left\| \Delta\bar{u}(k+j-1) \right\|_{\bar{R}}^2 = \left\| \Delta T(k+j-1) \right\|_{\bar{R}_1}^2 \quad (13)$$

So far, it can be found that the optimization objective (11) is equivalent to the following formula:

$$\bar{J}(k) = \sum_{j=1}^{M_y} \left\| S_{sp}(k+j) - S(k+j) \right\|_{Q_1}^2 + \sum_{j=2}^{M_u} \left\| \Delta T(k+j-1) \right\|_{R_1}^2 \quad (14)$$

For boundary conditions, there are similar transformations. According to the literature, the boundary constraints of input and output can be re-transformed as follows:

$$K \begin{bmatrix} \Delta\bar{u}(k) \\ \Delta\bar{u}(k+1) \\ \vdots \\ \Delta\bar{u}(k+M_u-1) \end{bmatrix} \leq L \quad (15)$$

Therefore, using formula (8), when n_1=1, formula (15)) can be transformed as follows:

$$K \begin{bmatrix} P\Delta T^T(k) \\ P\Delta T^T(k+1) \\ \vdots \\ P\Delta T^T(k+M_u-1) \end{bmatrix} \leq L \quad (16)$$

$$K \begin{bmatrix} P & \cdots & 0 \\ \vdots & \ddots & \vdots \\ 0 & \cdots & P \end{bmatrix} \begin{bmatrix} \Delta T^T(k) \\ \Delta T^T(k+1) \\ \vdots \\ \Delta T^T(k+M_u-1) \end{bmatrix} \leq L$$

$$K_1 \begin{bmatrix} \Delta T^T(k) \\ \Delta T^T(k+1) \\ \vdots \\ \Delta T^T(k+M_u-1) \end{bmatrix} \leq L$$

Finally, a constraint similar to constraint (5) can be obtained, that is, for the cost function (14), there are the following corresponding equivalent constraints:

$$\begin{cases} T_{min} \leq T(k+j) \leq T_{max} \\ \Delta T_{min} \leq \Delta T(k+j) \leq \Delta T_{max} \\ S_{min} \leq S(k+j) \leq S_{max} \end{cases} \quad (17)$$

In general, with the optimization index (14) and the corresponding ARX model, model predictive control can be performed. For example, if the above ARX model is assumed to be $j_a = j_b = 1$, then $s_i(k+1) = A_i S_i(k) + B_i t_i(k)$, where A_i and B_i can be obtained by Hi. From this, it can be obtained that under the process that the prediction period is a whole period:

$$\bar{s}_i(k) = F_i s_i(k) + G_i \bar{t}_i(k)$$

Among them,

$$\bar{s}_i(k) = \begin{Bmatrix} s_i(k+1) \\ s_i(k+2) \\ \vdots \\ s_i(k+N) \end{Bmatrix}, \bar{t}_i(k) = \begin{Bmatrix} t_i(k) \\ t_i(k+1) \\ \vdots \\ t_i(k+N-1) \end{Bmatrix}, F_i = \begin{bmatrix} A_i \\ A_i^2 \\ \vdots \\ A_i^N \end{bmatrix}, G_i$$
$$= \begin{bmatrix} B_i & 0 & \cdots & 0 \\ A_i B_i & B_i & \cdots & 0 \\ \vdots & \vdots & \ddots & \vdots \\ A_i^{N-1} B_i & A_i^{N-2} B_i & \cdots & B_i \end{bmatrix}$$

Then, the corresponding optimization of each MPC can be obtained from the above formula:

$$\min_{t_i} \frac{1}{2} \bar{t}_i{}^T(k) H_i \bar{t}_i(k) + s_i{}^T(k) L_i^T \bar{t}_i(k)$$

Among them,

$$H_i = 2G_i^T \bar{Q} G_i, L_i = 2G_i^T \bar{Q}_1 F_i$$

$$\bar{Q}_1 = diag\{Q_1, \cdots, Q_1, 0\} \bar{R} = diag\{R_1, \cdots, R_1, R_1\}$$

From this, rolling optimization can obtain the variable T needed each time. However, at the same time this is a special case of $j_a = j_b = 1$. When encountering practical problems, it may be necessary to reconstruct an appropriate QP problem analytical formula for the overall solution.

In order to explore the incentives and make the system have a certain robust performance, a certain extension is made in the system (2), and only the input and output data are used at the same time, so the system can be applied as:

$$x(k+1) = \bar{A}x(k) + \bar{B}\bar{u}(k) + \bar{\omega}(k)$$
$$\bar{y}(k) = \bar{C}x(k) + \bar{D}\bar{u}(k) + \bar{v}(k) \quad (18)$$

When the system is expected to be a stable closed-loop system, the system identification can be more precise. Therefore, a Kalman filter gain matrix K based on system (18) is set. Formula (18) is also equivalent to formula (19).

$$\hat{x}(k+1) = \bar{A}\hat{x}(k) + \bar{B}\bar{u}(k) + K\bar{e}(k)$$
$$\bar{y}(k) = \bar{C}x(k) + \bar{D}\bar{u}(k) + \bar{e}(k) \quad (19)$$

Among them, e(k) is the white noise residual irrelevant to the input and output. Compared with the data reorganization method (6) in the previous section, this subsection uses the following method to reorganize the data, and defines the following variable transformations:

$$\bar{u}_{s,k} = \begin{bmatrix} \bar{u}(k) \\ \vdots \\ \bar{u}(k+s-1) \end{bmatrix}, \bar{y}_{s,k} = \begin{bmatrix} \bar{y}(k) \\ \vdots \\ \bar{y}(k+s-1) \end{bmatrix},$$
$$\bar{\omega}_{s,k} = \begin{bmatrix} \bar{\omega}(k) \\ \vdots \\ \bar{\omega}(k+s-1) \end{bmatrix}, \bar{v}_{s,k} = \begin{bmatrix} \bar{v}(k) \\ \vdots \\ \bar{v}(k+s-1) \end{bmatrix}, \bar{e}_{s,k} = \begin{bmatrix} \bar{e}(k) \\ \vdots \\ \bar{e}(k+s-1) \end{bmatrix} \quad (20)$$

Similarly, the classical method based on subspace identification defines the input and output, residual, noise Hankel matrix and extended state vector in the case of N sets of data as follows:

$$\begin{aligned} \bar{U}_{k,s} &= [\bar{u}(s,k) \quad \cdots \quad \bar{u}(s,k+N-1)] \\ \bar{Y}_{k,s} &= [\bar{y}(s,k) \quad \cdots \quad \bar{y}(s,k+N-1)] \\ \bar{E}_{k,s} &= [\bar{e}(s,k) \quad \cdots \quad \bar{e}(s,k+N-1)] \\ \bar{W}_{k,s} &= [\bar{w}(s,k) \quad \cdots \quad \bar{w}(s,k+N-1)] \\ \bar{V}_{k,s} &= [\bar{v}(s,k) \quad \cdots \quad \bar{v}(s,k+N-1)] \\ \bar{X}_{k,s} &= [\bar{x}(s,k) \quad \cdots \quad \bar{x}(s,k+N-1)] \\ \hat{X}_{k,s} &= [\hat{x}(s,k) \quad \cdots \quad \hat{x}(s,k+N-1)] \quad (21) \end{aligned}$$

In order to facilitate future model predictive control and also meet the needs of subspace identification, the data collected in the above process is divided into past step lengths and future step length intervals. If we define s_p as the past time period step and s_f as the future time period step, then for formula (21), we can have the following transformations:

$$\bar{U}_p = \bar{U}_{k-s_p,s_p}, \bar{Y}_p = \bar{Y}_{k-s_p,s_p}, \bar{E}_p = \bar{E}_{k-s_p,s_p}, \bar{W}_p = \bar{W}_{k-s_p,s_p}, \bar{V}_p = \bar{V}_{k-s_p,s_p}$$
$$\bar{U}_f = \bar{U}_{k-s_f,s_f}, \bar{Y}_f = \bar{Y}_{k-s_f,s_f}, \bar{E}_f = \bar{E}_{k-s_f,s_f}, \bar{W}_f = \bar{W}_{k-s_f,s_f}, \bar{V}_f = \bar{V}_{k-s_f,s_f} \quad (22)$$

Then, by rearranging the above system, combining system (18) with formulas (21), (22), the following data-driven system model can be obtained:

$$\begin{aligned} \hat{Y}_f &= \wedge_f X_{k,1} + H_{u,f}\bar{U}_f + \Phi_f \\ \Phi_f &= H_{\omega,f} + \hat{V}_f \quad (23) \end{aligned}$$

The system matrix parameters are as follows:

$$\wedge_f = \begin{bmatrix} \bar{C} \\ \bar{C}\bar{A} \\ \vdots \\ \bar{C}\bar{A}^{s_f-1} \end{bmatrix}, H_{u,f} = \begin{bmatrix} \bar{D} & 0 & \cdots & 0 \\ \bar{C}\bar{B} & \bar{D} & \cdots & 0 \\ \vdots & \vdots & \ddots & \vdots \\ \bar{C}\bar{A}^{s_f-2} & \bar{C}\bar{A}^{s_f-3} & \cdots & \bar{D} \end{bmatrix},$$
$$H_{\omega,f} = \begin{bmatrix} 0 & 0 & \cdots & 0 \\ \bar{C}\bar{B} & \bar{D} & \cdots & 0 \\ \vdots & \vdots & \ddots & \vdots \\ \bar{C}\bar{A}^{s_f-2} & \bar{C}\bar{A}^{s_f-3} & \cdots & 0 \end{bmatrix} \quad (24)$$

Similarly, for the equivalent system (19) of system (18), it also has a similar implementation as follows:

$$\hat{Y}_f = \wedge_f \hat{X}_{k,1} + H_{u,f}\bar{U}_f + H_{e,f}\bar{E}_f \quad (25)$$

The system matrix parameters are as follows:

$$H_{e,f} = \begin{bmatrix} I & 0 & \cdots & 0 \\ \bar{C}\bar{B} & I & \cdots & 0 \\ \vdots & \vdots & \ddots & \vdots \\ \bar{C}\bar{A}^{s_f-2} & \bar{C}\bar{A}^{s_f-3} & \cdots & I \end{bmatrix} \quad (26)$$

In order to perform closed-loop subspace identification, a stable controller is added to the system (18) to make it stable, and has some properties of closed-loop poles, then like the dynamic output controller designed in Chapter 2, the following method is given:

$$\hat{x}(k+1) = \bar{A}_K\hat{x}(k) + \bar{B}_k\big(\bar{r}(k) - \bar{y}(k)\big)$$
$$\bar{u}(k) = \bar{C}_K\bar{x}(k) + \bar{D}_K\big(\bar{r}(k) - \bar{y}(k)\big) \quad (27)$$

where r is the expansion pattern of the signal to be tracked, and the relationship between the output and the input obtained from the previous formula. Then, by combining the controller (27) and equations (24) to (26), another form corresponding to the input and output can be obtained:

$$\hat{U}_f = \widetilde{\Lambda}_f\,\tilde{X}_{k,1} + \widetilde{H}_{u,f}\bar{R}_f + \widetilde{H}_{u,f}\bar{Y}_f \quad (28)$$

Among them, $\bar{R}_f = \bar{R}_{k,s_f} = \big[\bar{r}(s_f,k) \quad \cdots \quad \bar{r}(s_f,k+N-1)\big]$. The other parameter matrices have a similar form to formula (24), so I won't go into details here.

By combining formula (28) with formula (23), we get:

$$\bar{Y}_f = \Lambda_f\,X_{k,1} + \widetilde{H}_{u,f}\,\widetilde{\Lambda}_f\,\tilde{X}_{k,1} + H_{u,f}\widetilde{H}_{u,f}\bar{R}_f - H_{u,f}\widetilde{H}_{u,f}\bar{Y}_f + \Phi_f \quad (29)$$

If $G_f = 1 + H_{u,f}\widetilde{H}_{u,f}$,then:

$$G_f\bar{Y}_f = \Lambda_f\,X_{k,1} + H_{u,f}\,\widetilde{\Lambda}_f\,\tilde{X}_{k,1} + H_{u,f}\widetilde{H}_{u,f}\bar{R}_f + \Phi_f \quad (30)$$

Furthermore, we set the new variable M_f to have:

$$M_f = \widetilde{\Lambda}_f\,\tilde{X}_{k,1} + \widetilde{H}_{u,f}\bar{R}_f$$
$$= \bar{U}_f + \widetilde{H}_{u,f}\bar{Y}_f \quad (31)$$

Similarly, for the past time step, we have: (32)

From this, it can be seen that the following equation holds:

$$G_f\bar{Y}_f = \Lambda_f\,X_{k,1} + H_{u,f}M_f + \Phi_f \quad (33)$$

However, no explicit expression is given here, because it can be obtained from formula (5) in Chapter 2, and it can be known that $X_{k,1}$ has a certain linear relationship with M_p and $\bar{Y}_p$ due to iteration. At the same time, this vector matrix is taken LQ decomposition, which can have:

$$\begin{bmatrix} S_p \\ M_f \\ \bar{Y}_f \end{bmatrix} = \begin{bmatrix} L_{11} & 0 & 0 \\ L_{21} & L_{22} & 0 \\ L_{31} & L_{32} & L_{33} \end{bmatrix} \begin{bmatrix} Q_1 \\ Q_2 \\ Q_3 \end{bmatrix}, S_p = \begin{bmatrix} M_P \\ \bar{Y}_p \end{bmatrix} \quad (34)$$

From the LQ decomposition (34), it can be known that:

$$\bar{Y}_f = (L_{31}L_{11}^{-1} - L_{23}L_{22}^{-1}L_{21}L_{11}^{-1})S_p + L_{32}L_{22}^{-1}M_f + L_{33}Q_3 \quad (35)$$

Meanwhile, according to formula (33), there are:

$$\begin{aligned} G_f^{-1} \wedge_f X_{k,1} &= (L_{31}L_{11}^{-1} - L_{23}L_{22}^{-1}L_{21}L_{11}^{-1})S_p \\ G_f^{-1}H_{u,f} &= L_{32}L_{22}^{-1} \\ G_f^{-1}\Phi_f &= L_{33}Q_3 \quad (36) \end{aligned}$$

Then, by deriving formula (36), we can get:

$$G_f = \left(1 - L_{32}L_{22}^{-1}\bar{H}_{u,f}\right)^{-1} \quad (37)$$

Similarly, from $G_f = 1 + H_{u,f}\widetilde{H}_{u,f}$, it can be seen that:

$$G_f = \left(1 - L_{32}L_{22}^{-1}\bar{H}_{u,f}\right)^{-1} \quad (38)$$

Therefore, we can end up with the following result:

$$\wedge_f X_{k,1} = \left(1 - L_{23}L_{22}^{-1}\widetilde{H}_{u,f}\right)^{-1}(L_{31}L_{11}^{-1} - L_{23}L_{22}^{-1}L_{21}L_{11}^{-1})S_p \quad (39)$$

At this point, the system modeling can be carried out by formula (37) and formula (38).

However, for the model predictive controller to be designed in this section, system identification is not required, but formula (35) is directly used as the prediction model to design the model predictive controller. At the same time formula (35) can be equivalent to:

$$\hat{Y}_f = L_p S_p + H_{u,f}\bar{U}_f + G_f^{-1}\Phi_f \quad (40)$$

Among them, $\hat{Y}$, $\bar{U}_f$, and $\bar{U}_f$ are known input and output data, and other parameters can be obtained in the following ways.

$$L_p = \left(I - L_{32}L_{22}^{-1}\widetilde{H}_{u,f}\right)^{-1}(L_{31}L_{11}^{-1} - L_{32}L_{22}^{-1}L_{21}L_{11}^{-1})$$

$$H_{u,f} = \left(I - L_{32}L_{22}^{-1}\widetilde{H}_{u,f}\right)^{-1}L_{32}L_{22}^{-1}, G_f^{-1} = I - L_{32}L_{22}^{-1}\widetilde{H}_{u,f}$$

Among them, $\widetilde{H}_{u,f}$ is obtained when the initial controller is designed. The remaining relevant parameters are obtained by LQ decomposition of the input and output data.

Next, the design of the model predictive controller is carried out, and the performance indicators are defined:

$$\bar{J}(k) = \sum_{j=1}^{M_y} \|\bar{r}(k+j) - \bar{y}(k+j)\|_{\bar{Q}}^2 + \sum_{j=2}^{M_u} \|\Delta\bar{u}(k+j-1)\|_{\bar{R}}^2 \quad (41)$$

Its boundary conditions are: (42)

For this typical model predictive controller, after obtaining the predictive model through the input and output data, it can be easily transformed into a QP quadratic problem to solve according to the cost function. In this solution process, the input needs to be derived, but the Φ_f term is zero after the derivative.

3. Simulation description

This paper collects college students' exercise and nutritional intake data from colleges and universities, analyzes the relevant data, runs the system, and compares the output signals, as shown in Figure 2.

It can be clearly obtained from Figure 2 that the ARX model can well imitate the multi-rate sampling system and show the dynamic characteristics of the multi-rate sampling system.

At the same time, it can be seen from its convergence that under the condition of fixed input, the output y1 does not gradually converge to the steady-state value we need, but converges to 10.2mA. It shows that the linear model is a stable system, but in the case of no control rate, it cannot track our expected value.

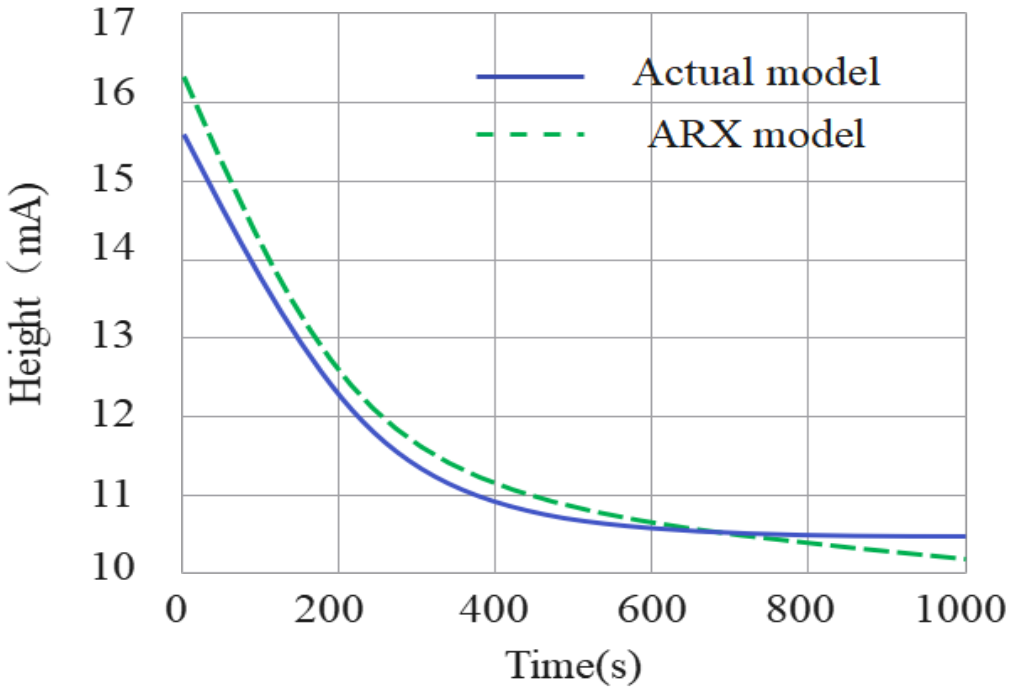

Figure 2. Comparison between multi-rate sampling system and ARX model

Next, Algorithm 1 is used to design a PLS-based data-driven model predictive controller. After running the system for more than 2000s to obtain

500 sets of data, after collecting the data and establishing the ARX model, this paper sets the initial state as x =[o.005635.22319.3]^T.

The goal of this experiment is to make the three output variables of this linear system track to the desired steady state, that is, $y_{sp} = [12 \quad 11.89 \quad 10.5]^T$. Running the system, the output tracking trajectory is obtained as shown in Figure 3.

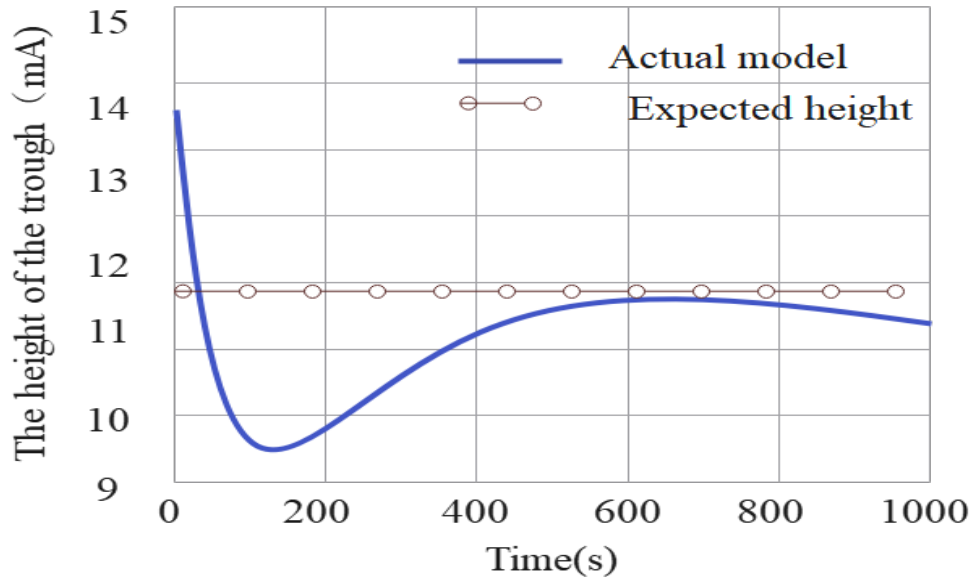

(a) Output y_1 tracking of CSTH model under PLS-based data-driven model predictive controller

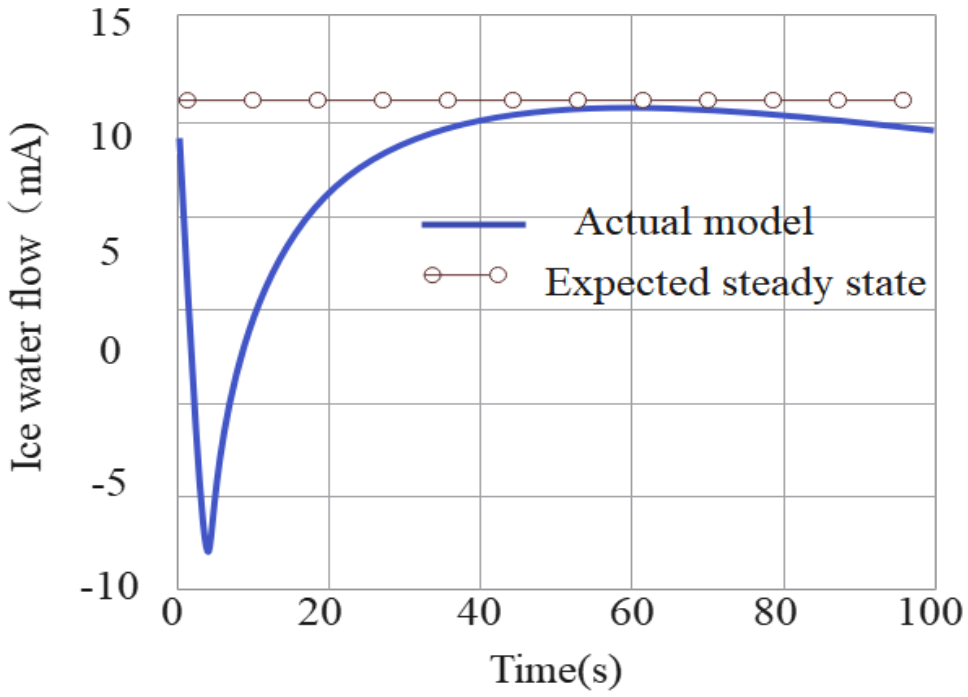

(b) Output y_2 tracking of CSTH model under PLS-based data-driven model predictive controller

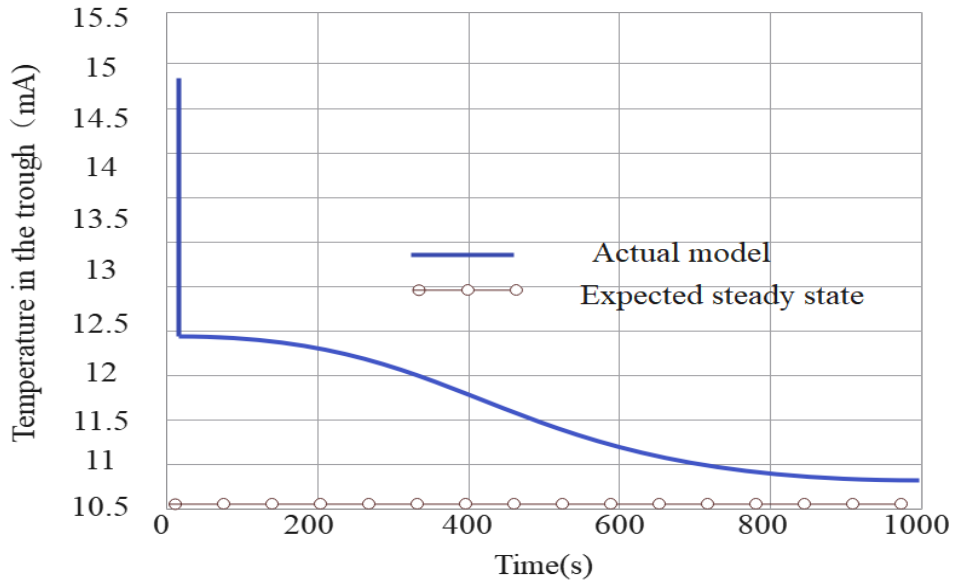

(c) Output y_3 tracking of CSTH model under PLS-based data-driven model predictive controller

Figure 3. Output of CSTH model under PLS-based data-driven model predictive controller

It can be seen from the figure that all states can be quickly tracked to the expected steady state. Compared to Figure 3 for a given fixed input, the output tracking speed increases sharply, also because the system input is not constrained.

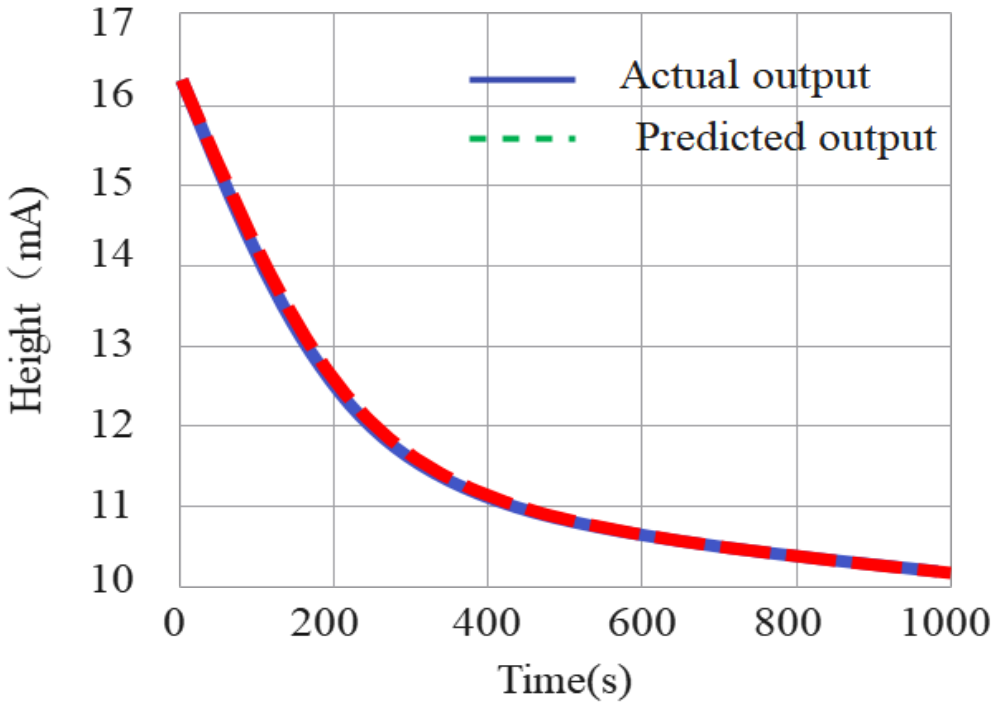

Figure 4. Comparison of actual output y_1 and predicted output based on subspace identification method

A full frequency domain controller is given whose main purpose is to

stabilize the system. The hyperparameters in the given algorithm are sp = 50, sf = 30, N = 5000. Then, according to Algorithm 2, a data-driven model predictive controller is designed. At the same time, it is compared with the data-driven controller based on the PLS method, so the linear model of nutrition intake and energy consumption in college students' exercise described in the paper is also used, such as (44).

Considering the same multi-rate sampling characteristics, the actual output and predicted output are verified as shown in Figure 4.

As can be seen from the above figure, both data-driven methods for obtaining the system prediction model can ensure that the error between the actual output and the predicted output is very small. The difference between the two is that the former prediction model is smooth but the error is slightly larger than the latter, while the latter prediction model has data noise interference but the error is smaller. However, this difference does not affect the model predictive control effect. Under the same initial conditions, the same optimization function, and the same constraints, the output changes are different but very close.

Therefore, there is not much proof given in the current verification process. The system described in the paper considered here has certain limitations. In this case, the initial value of the given system is $x = [0.005635.22319.3]^T$.

The steady state is expected to remain unchanged. The output tracking of the multi-rate sampling system under the data-driven controller method based on subspace identification can be obtained as shown in Figure 5.

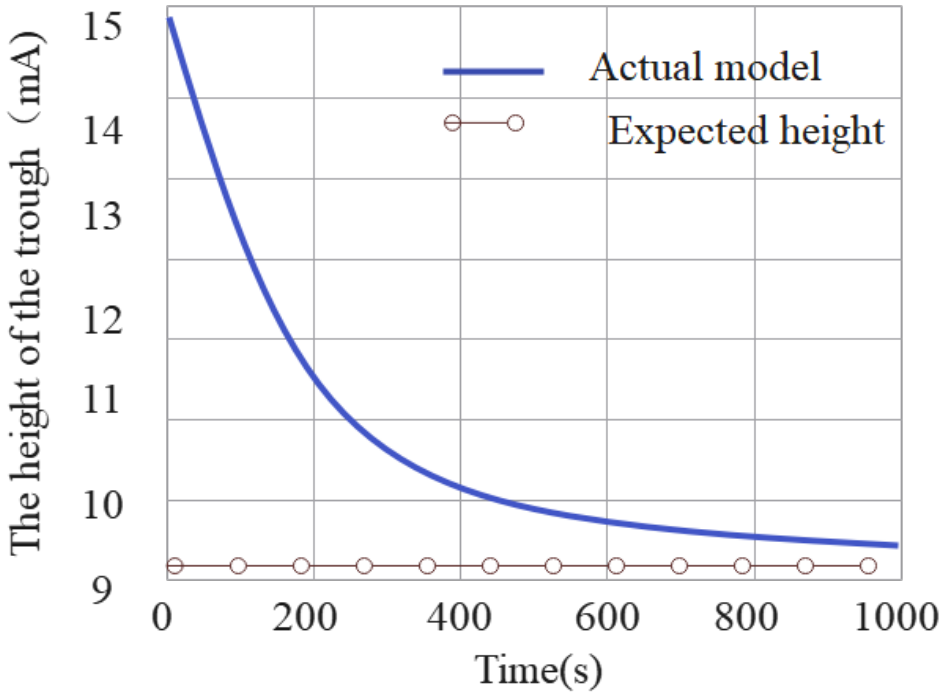

(a) Output y_1 tracking of CSTH model under PLS-based data-driven model predictive controller

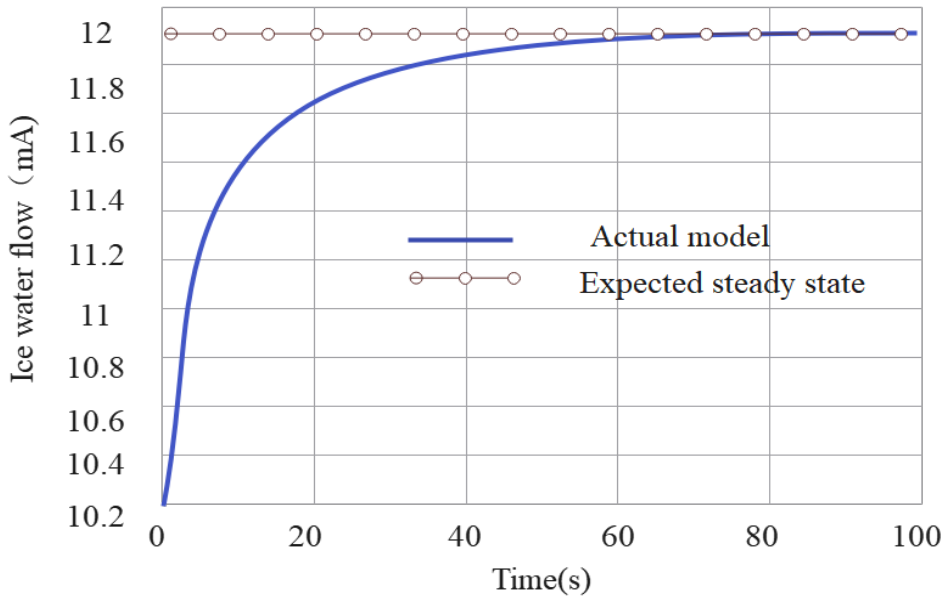

(b) Output y_2 tracking of CSTH model under PLS-based data-driven model predictive controller

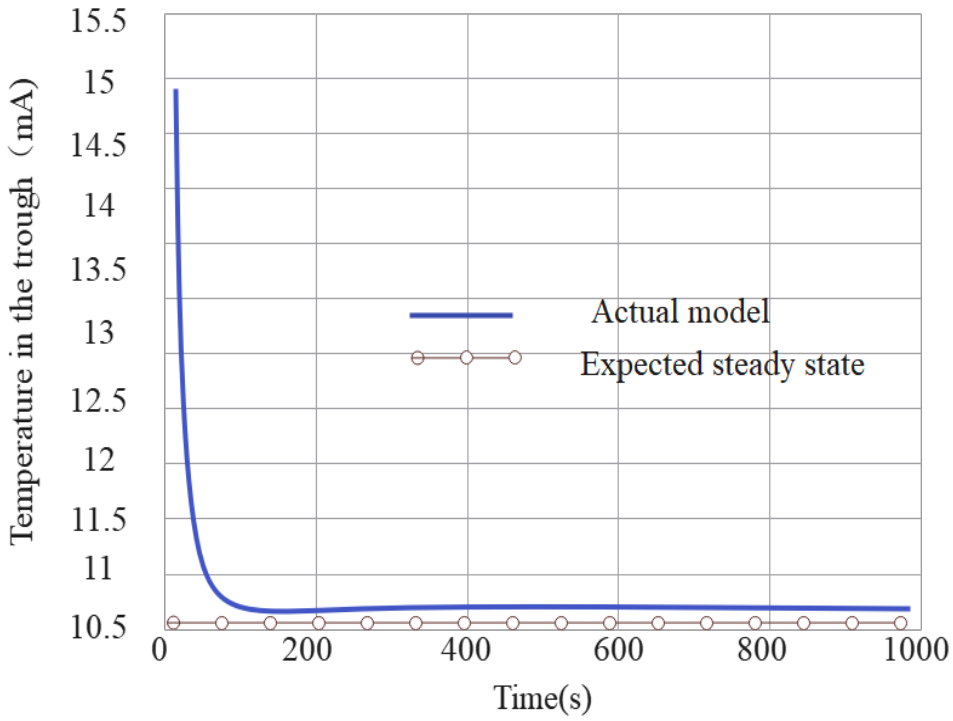

(c) Output y_3 tracking of CSTH model under PLS-based data-driven model predictive controller

Figure 5. Output of CSTH model under PLS-based data-driven model predictive controller

After the above simulations, it can be proved that Algorithm 2, that is, the multi-rate sampling system based on subspace identification, can well model the prediction model of nutrition involvement and energy consumption in college students' exercise, and then perform predictive control.

Most of the energy materials required by college students in the process of exercising are obtained from external nutrients, and then released, transferred and utilized in the body to provide the energy needed for the body to exercise. The balanced and comprehensive nutrition of college athletes is related to the performance of athletes' physical functions, the state of competition and the recovery of fatigue after exercise. Moreover, each nutrient plays a unique role in the process of exercise, providing a solid material basis for the physical function of athletes.

During the whole stage of exercise, including before, during, and after exercise, the supplementation of reasonable nutrients is the guarantee for athletes to play their outstanding skills and the premise for creating excellent sports performance. After training and competition, college athletes can do stretching or massage collectively, which can relieve physical fatigue as soon as possible, and also have a certain promotion effect on the recovery of energy in the body. Therefore, in addition to paying attention to the physical quality and sports performance of college students, teachers should also pay attention to the dietary nutrition of the team members.

They should give dietary advice to different team members, and at the same time, they should enrich the nutritional knowledge of athletes. College students should supplement energy according to their own conditions and reference values. Only scientific diet can achieve the best energy supplement effect and tap the greatest physical potential.

4. Conclusion

At the university stage, the management from schools and families is gradually relaxed, and the educational level of different students is not the same before entering university, and many students do not develop independent world outlook and values after entering university. Therefore, they lack basic judgment and flexible problem-solving ability for various difficulties that may arise in life.

Moreover, many students lack sleep, cannot develop a scientific schedule, are addicted to the Internet and games, and do not pay attention to personal hygiene. At the same time, they do not have enough understanding of nutrition and health knowledge and basic dietary matching, and gradually form a variety of unhealthy lifestyles such as smoking and excessive drinking. In addition, because some students are young and energetic, it is difficult for some students to face and deal with problems calmly. The boring nutrition knowledge courses and the earnest teaching of parents and elders may not achieve the desired effect.

Therefore, how to formulate nutrition education strategies for different students to improve students' physical fitness and nutritional status is particularly important. This paper combines big data technology to analyze the nutritional intake and energy consumption of college students in sports, and promotes the balance of nutritional intake and energy consumption in the process of college students' sports. Finally, this paper verifies the validity of the model in this paper through experimental research.

References

Altwaijry, N., El-Masry, T. A., Alotaibi, B., Tousson, E., & Saleh, A. (2020). Therapeutic effects of rocket seeds (Eruca sativa L.) against testicular toxicity and oxidative stress caused by silver nanoparticles injection in rats. *Environmental toxicology, 35*(9), 952-960.

Arman, M. S. I., Al Mahmud, A., Mahmud, H. R., & Reza, A. A. (2019). Free radical, oxidative stress and diabetes mellitus: A mini review. *Discovery Phytomedicine, 6*(3), 99-101.

Benzer, F., Kandemir, F. M., Kucukler, S., Comaklı, S., & Caglayan, C. (2018). Chemoprotective effects of curcumin on doxorubicin-induced nephrotoxicity in wistar rats: by modulating inflammatory cytokines, apoptosis, oxidative stress and oxidative DNA damage. *Archives of physiology and biochemistry, 124*(5), 448-457.

Beyfuss, K., & Hood, D. A. (2018). A systematic review of p53 regulation of oxidative stress in skeletal muscle. *Redox Report, 23*(1), 100-117.

Choi, S., Liu, X., & Pan, Z. (2018). Zinc deficiency and cellular oxidative stress: prognostic implications in cardiovascular diseases. *Acta pharmacologica Sinica, 39*(7), 1120-1132.

Daenen, K., Andries, A., Mekahli, D., Van Schepdael, A., Jouret, F., & Bammens, B. (2019). Oxidative stress in chronic kidney disease. *Pediatric nephrology, 34*, 975-991.

Dzik, K. P., & Kaczor, J. J. (2019). Mechanisms of vitamin D on skeletal muscle function: oxidative stress, energy metabolism and anabolic state. *European journal of applied physiology, 119*, 825-839.

Feng, P., Ye, Z., Han, H., Ling, Z., Zhou, T., Zhao, S., . . . El-Dalatony, M. M. (2020). Tibet plateau probiotic mitigates chromate toxicity in mice by alleviating oxidative stress in gut microbiota. *Communications biology, 3*(1), 242.

Forman, H. J., & Zhang, H. (2021). Targeting oxidative stress in disease: Promise and limitations of antioxidant therapy. *Nature Reviews Drug Discovery, 20*(9), 689-709.

Garza-Lombó, C., Posadas, Y., Quintanar, L., Gonsebatt, M. E., & Franco, R. (2018). Neurotoxicity linked to dysfunctional metal ion homeostasis and xenobiotic metal exposure: redox signaling and oxidative stress. *Antioxidants & redox signaling, 28*(18), 1669-1703.

Hassanzadeh, K., & Rahimmi, A. (2019). Oxidative stress and neuroinflammation in the story of Parkinson's disease: could targeting these pathways write a good ending? *Journal of cellular physiology, 234*(1), 23-32.

Kruk, J., Aboul-Enein, H. Y., Kładna, A., & Bowser, J. E. (2019). Oxidative stress in biological systems and its relation with pathophysiological functions: the effect of physical activity on cellular redox homeostasis. *Free radical research, 53*(5), 497-521.

Kurucz, V., Krüger, T., Antal, K., Dietl, A.-M., Haas, H., Pócsi, I., . . . Emri, T. (2018). Additional oxidative stress reroutes the global response of Aspergillus fumigatus to iron depletion. *BMC genomics, 19*, 1-19.

Olechnowicz, J., Tinkov, A., Skalny, A., & Suliburska, J. (2018). Zinc status is associated with inflammation, oxidative stress, lipid, and glucose metabolism. *The journal of physiological sciences, 68*(1), 19-31.

Qi, J.-h., & Dong, F.-x. (2021). The relevant targets of anti-oxidative stress: a review. *Journal of drug targeting, 29*(7), 677-686.

Wei, L., Lu, X., Kang, X., & Song, Y. (2020). Determination of glutathione and cysteine in human breast milk by high-performance liquid chromatography with chemiluminescence detection for evaluating the oxidative stress and exposure to heavy metals of lactating women. *Analytical Letters, 53*(16), 2607-2618.

Xi, J., Luo, X., Wang, Y., Li, J., Guo, L., Wu, G., & Li, Q. (2019). Tetrahydrocurcumin protects against spinal cord injury and inhibits the oxidative stress response by regulating FOXO4 in model rats. *Experimental and therapeutic medicine, 18*(5), 3681-3687.